UNSTEADY LOSS IN THE STATOR DUE TO THE INCOMING ROTOR WAKE IN A HIGHLY-LOADED TRANSONIC COMPRESSOR

Chunill Hah

NASA Glenn Research Center
21000 Brookpark Road
Cleveland, Ohio 44135

ABSTRACT

The present paper reports an investigation of unsteady loss generation in the stator due to the incoming rotor wake in an advanced GE transonic compressor design with a high-fidelity numerical method. This advanced compressor with high reaction and high stage loading has been investigated both experimentally and analytically in the past. The measured efficiency in this advanced compressor is significantly lower than the design intention/goal. The general understanding is that the current generation of compressor design/analysis tools miss some important flow physics in this modern compressor design. To pinpoint the source of the efficiency miss, an advanced test with a detailed flow traverse was performed for the front one and a half stage at the NASA Glenn Research Center. Detailed data-match analysis by GE identified an unexpected high loss generation in the pressure side of the stator passage. Higher total temperature and lower total pressure are measured near the pressure side of the stator. Various analyses based on the RANS and URANS of the compressor stage do not calculate the measured higher total temperature and lower total pressure on the pressure side of the stator. In the present paper, a Large Eddy Simulation (LES) is applied to find the fundamental mechanism of this unsteady loss generation in the stator due to the incoming rotor wake. The results from the LES were first compared with the NASA test results and the GE interpretation of the test data. LES calculates lower total pressure and higher total temperature on the pressure side of the stator, as the measured data showed, resulting in large loss generation on the pressure side of the stator. Detailed examination of the unsteady flow field from LES shows that the rotor wake, which has

higher total temperature and higher total pressure relative to the free stream, interacts quite differently with the pressure side of the blade compared to the suction side of the blade. The higher temperature in the wake remains high as the wake passes through the pressure side of the blade. On the other hand, the total temperature diffuses as it passes through near the suction surface. For the presently investigated compressor, the classical intra-stator wake transport to the pressure side of the blade by the slip velocity in the wake seems to be minor. The main causes of this phenomenon are three-dimensional unsteady vortex interactions near the blade surface. The stabilizing effect of the concave curvature on the suction side keeps the rotor wake thin. On the other hand, the destabilizing effect of the convex curvature of the pressure side makes the rotor wake thicker, which results in a higher total temperature measurement at the stator exit. Additionally, wake stretching through the stator seems to contribute to the redistribution of the total temperature and the loss generation.

INTRODUCTION

Many significant studies have been reported on loss generation inside multi-stage compressors. Smith [1966] explained that rotor wake stretching in the stator provides some total pressure recovery in his widely referenced classical paper. Van Zante et al. [2002] examined this wake recovery effect in a high speed axial compressor. Kerrebrock and Mikolajczk [1970] reported that the rotor wake, which has higher total pressure and higher total temperature in absolute frame than fluid in the free stream, is transported to the pressure side of the stator due to the slip velocity in the stator frame.

RANS and URANS have been widely used for the design and analysis of compressor/turbine
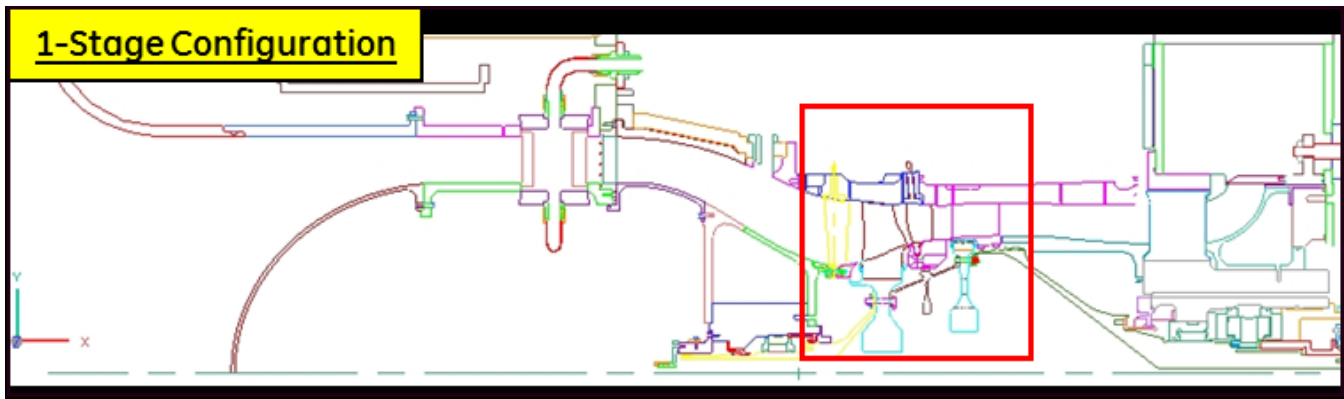
Figure 1: 1-Stage Rig Configuration

stages. A 1-2% efficiency improvement is attributed to these analysis tools (Smith [2010]). However, recent studies (for example, Hah and Katz [2014]) found that the generation, transport, and interactions of vortices in turbomachinery are not well calculated by RANS and URANS. Modeling of all the turbulence scales in the entire field with a single length scale might be one of reasons for this behavior. Recently, higher fidelity analysis tools based on Direct Numerical simulation (DNS) and LES are being introduced for turbomachinery flow analysis (Zaki et al. [2010], Hah et al. [2012], Gourdain [2013], Hah and Katz [2014], and Papadogiannis et al. [2014]).

To increase the efficiency of large gas turbine engines, advanced high pressure ratio core compressors with fewer stages have been designed and tested recently. Although these compressors were designed with the current state-of-the-art design technology, the measured stage efficiencies were much lower than the design intention. Various types of Reynolds-averaged Navier-Stokes analyses (RANS) for the multi-stage configuration and full unsteady Reynolds-averaged Navier-Stokes analysis (URANS) are used in the current design process. Consequently, it has been suggested that some of the flow physics inside such a highly-loaded compressor stage are not properly captured with these analytical tools.

A test was performed at the NASA Glenn Research Center to pinpoint the source of loss with an advanced GE compressor design. The results, reported by Prahst et al. [2015], show that front stage efficiency is significantly lower than RANS and URANS calculations. Evaluation and detailed data match analysis of the measured data are reported by Lurie and Breeze-Stringfellow [2015]. The measured data shows that a large loss is generated on the pressure side of the stator. A higher total temperate and a lower total pressure were measured on the pressure side of the stator. The current generation of RANS and URANS misses this large loss generation. A LES simulation of this flow field with a relatively fine grid calculates this
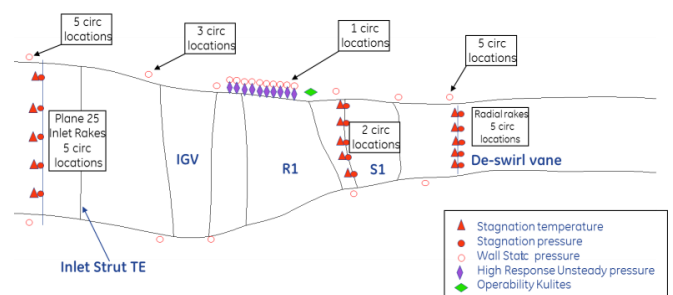

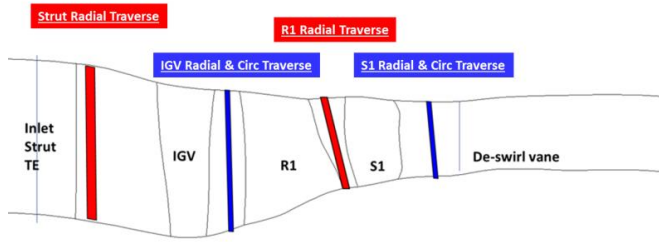**Figure 2: Inter-Stage Aero Instrumentation**
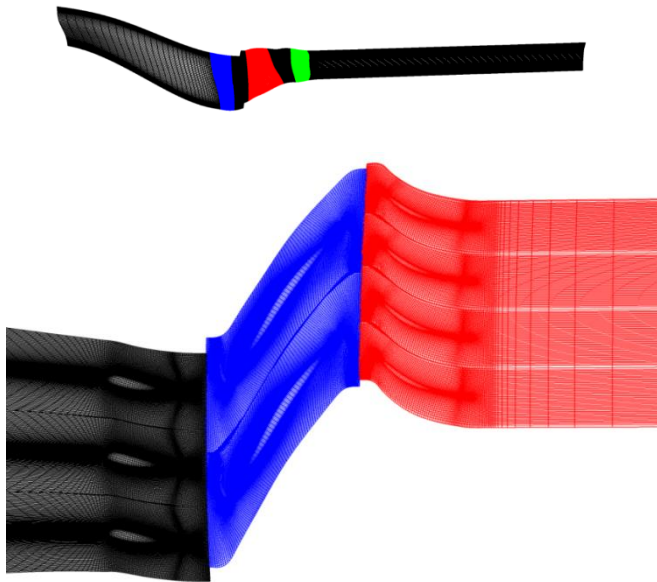
Figure 3: Traversing Instrumentation

Figure 4: Computational domain and grid topology

large loss generation fairly well (Hah [2015]). The current paper is aimed to identify the basic mechanism of this unsteady loss generation.

TEST DATA AND LES SETUP

Figure 1 shows the single stage test rig configuration. For the NASA investigation of the GE highly-loaded axial compressor, aero tests were performed for the first stage alone and the first two-stage configuration. The present LES analysis was performed for the 1-stage setup, which consisted of the Strut, IGV, Rotor 1, and Stator 1. Aero

instrumentation and stage traversing instrumentation are shown in Figures 2 and 3. The traverses in Figure 3 consisteted of a 5–hole probe, stagnation Kulite probes, and hotwire probes to perform radial and circumferential traverses behind the IGV, Rotor 1 (R1) and Stator 1 (S1). Additionally, various fixed inter-stage instrumentation, including over-the-rotor Kulite and S1 leading edge total pressure and total temperature probes, were installed. Details of the test, data aquistion and data interpretation are given by Prahst et al. [2015] and Lurie and Breeze-Stringfellow [2015].

Figure 4 shows the computational domain and the grid topology for the LES analysis. The exit plane of the computational domain was placed about 10 S1 blade heights away to minimize pressure reflection from the exit plane. The inlet plane was located near the inlet strut trialing edge. Details of the LES process are given by Hah and Shin. [2012]. The subgrid stress tensor was modeled with the standard dynamic model by Germano et al. [1991]. A third-order accurate interpolation scheme is used for the convection term.

As is well known (for example, Padogiannis et al. [2014]), the LES solution depends on the grid size and requires much longer computation than URANS. To get a converged unsteady flow field in a single-stage compressor with URANS, the computation of 20 – 30 rotor revolutions might be required. On the other hand, LES might require as much as 100 - 200 rotor revolutions to obtain the periodic unsteady flow field. The influence of different models of the subgrid scale stress becomes less recognizable when the computational grid becomes finer. Susequently, the user's understanding and experience with any particular LES procedure are still very important factors in extracting useful physical insights from the LES simulation.

The actual number of blades in the current compressor is 42 IGV blades, 28 rotor blades, and 58 stator blades. To perform fine grid LES simulations of the stage with periodicity conditons in the tangential direction, the number of stator blades was changed to 56 by scaling the stator
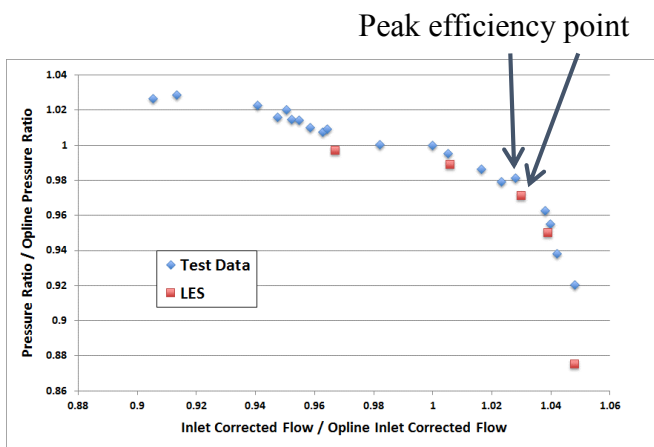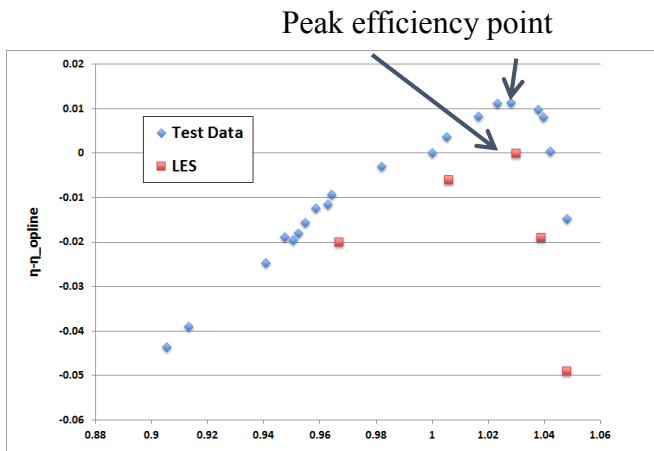
Peak efficiency point

Figure 6: Instantaneous pressure distribution at mid-span

Peak efficiency point

Figure 5: Comparison of corrected speedline relative to multi-stage compressor opline
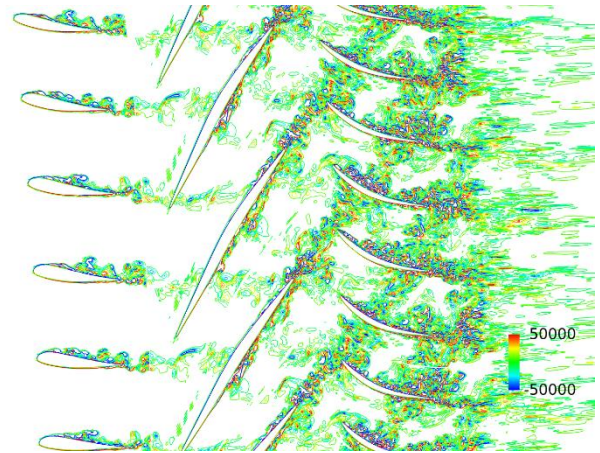
Figure 7: Instantaneous vorticity contours at mid-span

blade. LES was performed with 3 IGV blades, 2 rotor blades and 4 stator blades, which represents 1/14 of the machine passage. Various sizes of the computational grid were tested for the LES simulation. LES with 150 million grid nodes for the 9 blade passages (3 IGV + 2 R1 + 4 S1) does not calculate the measured high loss region on the pressure side of the stator. It was found that the total size of more than 300 million CFD nodes for the 9 blade passages is necessary to calculate the observed loss generation in the stator passage. The calculated LES flow field with 460 million CFD nodes were compared with the measured data in the previous paper (Hah [2015]). The main focus 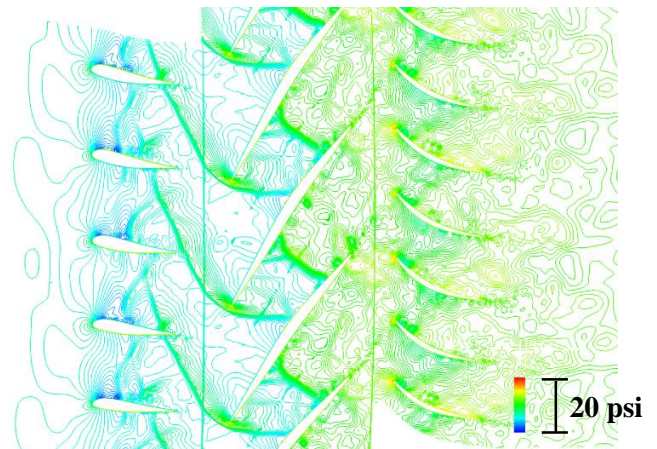of the current paper is to identify the fundamental flow mechnaism of the unexpected high loss generation in the stator's pressure side by examining the unsteady flow field from LES.

All the computations were performed with NASA's Pleiades supercomputer system. With the 960 parallel processors, about 60 CPU hours are required for each compressor rotor revolution with the fine CFD grid.

COMPRESSOR SPEEDLINE AND OVER ALL FLOW FIELD

Detailed comparisons between the LES and the measured data for the compressor performance were made in the previous paper (Hah [2015]). Overall characteristics are briefly described here.
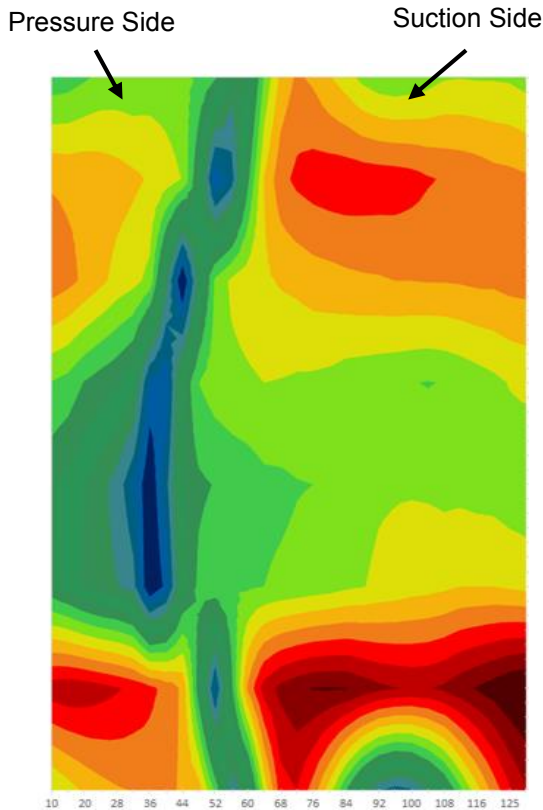
4

Pressure Side   Suction Side

10 20 28 36 44 52 60 68 76 84 92 100 108 116 125

Figure 8: Measured total pressure at the stator exit

Pressure Side   Suction Side

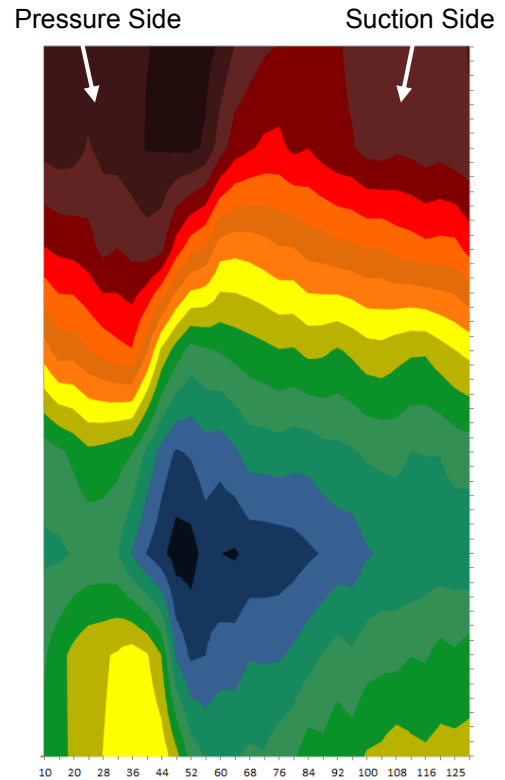10 20 28 36 44 52 60 68 76 84 92 100 108 116 125

Figure 9: Measured total temperature at the stator exit

Figure 5 shows the measured and the calculated corrected speedline of the compressor stage. LES calculates a slightly higher choke mass flow rate than the measurement. The mass flow rate in Figure 5 was corrected by the mass flow rate corresponding to the opline of the full machine. LES calculates lower pressure rise and lower compressor efficiency compared to the measurement. However, the overall trend of the compressor characteristics seems to be calculated properly. An instantaneous pressure field at mid-span is shown in Figure 6. As expected with the high rotor blade loading, a strong flow interaction between the Rotor 1 shock and the IGV blade is shown in Figure 6.

Instantaneous vorticity contours at mid-span from the LES are shown in Figure 7. Effects of shock-induced vortices on performance in transonic compressors were investigated by Nolan et al. [2009] and Knobbe et al. [2013]. Both the

current LES and the GE data match analysis by Lurie and Breeze-Stringfellow [2015] show that the loss through the IGV is small. The vorticity contours in Figure 7 do not indicate any strong IGV wake phasing on the rotor. LES simulations with wider spaces between the IGV and Rotor 1 did not show any appreciable change in the rotor performance. The LES shows that about two thirds of the overall loss occurs through the Rotor 1 exit plane in Figure 1. The flow field in this compressor has been investigated extensively with several different stage configurations and accompanying analysis tools. Based on the current detailed inter-stage measurements, detailed data analysis (Lurie and Breeze-String Fellow [2015]), and the present LES simulation, additional loss, which was not identified previously with RANS and URANS, was determined to occur through the Stator 1 passage.
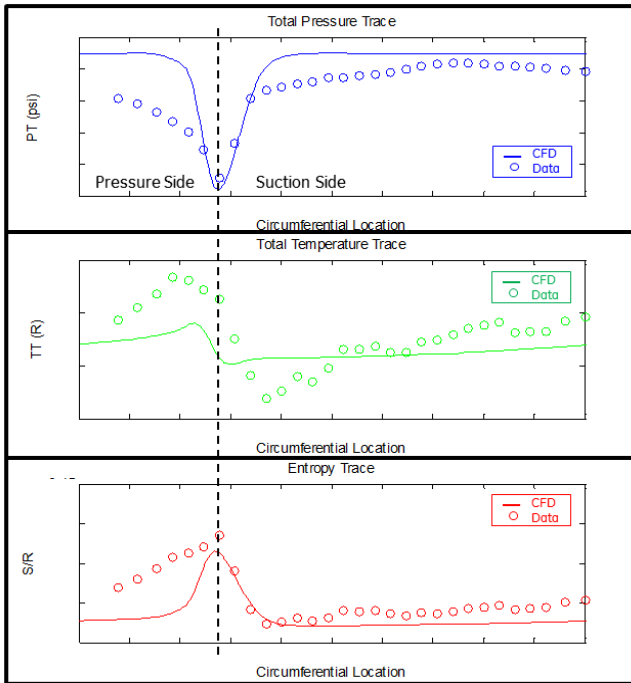
5

Figure 10: S1 TE Total pressure, total temperature, and entropy data vs CFD at 48.1% span (from Lurie and Breeze-Stringfellow [2015])

LOSS GENERATION THROUGH STATOR 1

The interaction of rotor wakes with stator blades in compressors has been studied extensively. Smith [1966] explained the effects of wake stretching through the stator passage. Kerrbrock and Mikolajcak [1970] showed that the rotor wake has a higher total temperature in the stator frame and accumulates on the pressure side of the stator.

Figures 8 and 9 show the measured distribution of total pressure and the total temperature at the exit of Stator 1. The total pressure distribution in Figure 8 shows lower total pressure on the pressure side of the blade between 20% and 80% of the span. On the other hand, the total temperature is higher on the pressure side than that on the suction side according to the measurement in Figure 9. Higher total temperature and lower total pressure on the pressure side means there is a higher loss generation on the pressure side, which was not expected previously. In Figure 10, pitchwise distributions of total pressure, total temperature,
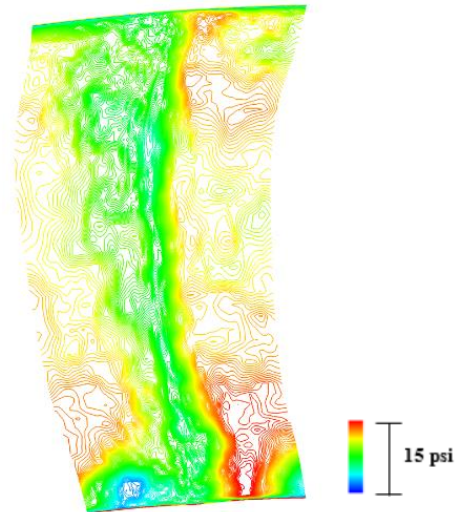

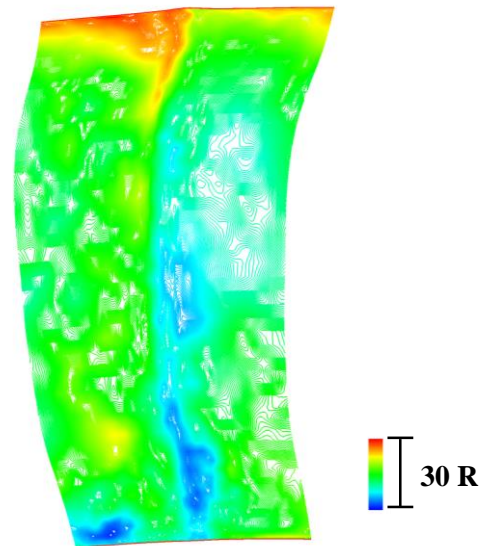**Figure 11: Total pressure distribution at stator exit from LES**

Figure 12: Total temperature distribution at stator exit from LES

and entropy are compared with the measurement and a stage RANS/URANS simulation (Lurie and Breeze-String Fellow [2015]). As mentioned earlier, the current generation of RANS/URANS misses large loss generation on the pressure side of the stator passage.

Distributions of total pressure and total temperature at the stator exit from the LES (460
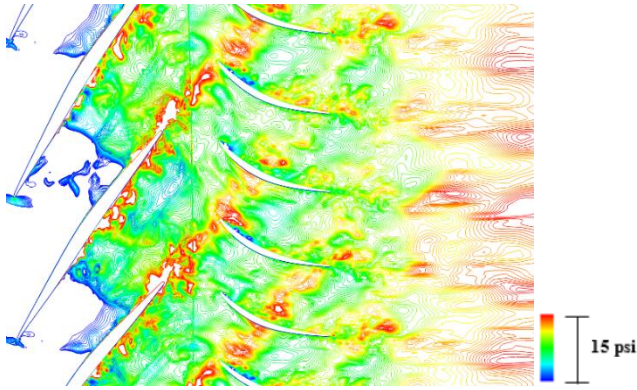
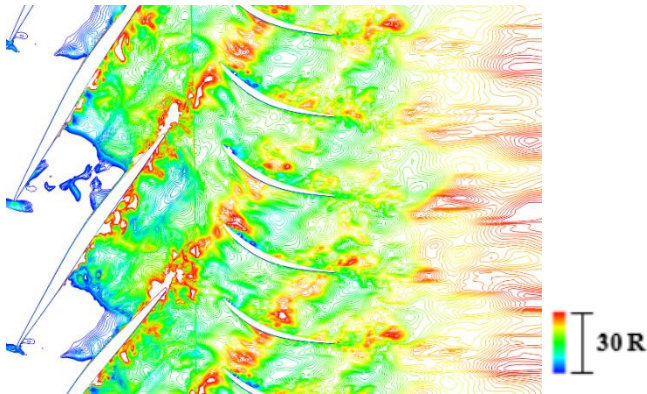**Figure 13: Instantaneous total pressure distribution at mid-span**

Figure 14: Instantaneous total temperature distribution at mid-span

million CFD nodes) are given in Figures 11 and 12. The results from this LES show higher total temperature and lower total pressure on the pressure side of the blade passage correctly. In the following sections, possible causes for the large loss generation on the pressure side of the stator are examined with the available measured data and LES with the fine computational grid.

Intra-stator Transport of Rotor Wake

Kerrbrock and Mikolajcak [1970] explained that the circumferential non-uniformity of total temperature distribution downstream of the stator in axial-flow compressors is due to intra-stator transport of the rotor wake. They pointed out that the rotor wake has a higher total temperature in the stator frame and accumulates on the pressure side of the stator. Figures 13 and 14 show instantaneous distribution of total pressure and total temperature in the stator frame. For this highly-loaded transonic compressor, both the total pressure and the total temperature are higher in the rotor wake. As shown in Figures 7 and 8, time-averaged total pressure is lower and the total temperature is higher near the pressure side of the passage at the stator exit. Figure 15 illustrates instantaneous relative velocity vectors in the rotor passage and absolute velocity vectors in the stator passage. The rotor wake fluid has an additional jet velocity component in the stator reference frame as shown in Figure 15. As shown by Kerrebrock and Mikolajczak [1970], this jet velocity pushes the wake fluid toward the pressure side of the blade. The instantaneous velocity vectors in Figure 15 show that the rotor wake consists of vortical structures and is not like the traditional two-dimensional inviscid wake.

Instantaneous distributions of the tangential velocity component are given in Figure 16. The tangential velocity component decays rapidly and becomes almost negligible after it enters the stator passage for the current compressor. Therefore, the intra-stator transport of the rotor wake due to the slip velocity may not be the main cause of the high total temperature near the pressure side of the stator. The intra-stator transport of the wake is an inviscid phenomenon. If the high temperature accumulation near the pressure side is due to this inviscid phenomenon, a simple stage URANS should pick up this phenomenon. It appears that URANS based on a fine grid or a LES based on a relatively coarse grid does not pick up this phenomenon. Therefore, this intra-stator transport of hot rotor wake might not be the main mechanism for the phenomenon.

In Figure 17, time-space plots of the total pressure at 48.1% span are shown. In Figure 17, the trace of the passing rotor 1 wake is clearly shown. In Figure 18, instantaneous distribution of the total pressure at three different times as the rotor wake passes through the stator is given. Total pressure distributions in Figures 17 and 18 do not show strong migration of the rotor wake toward the pressure side as it goes through the stator.
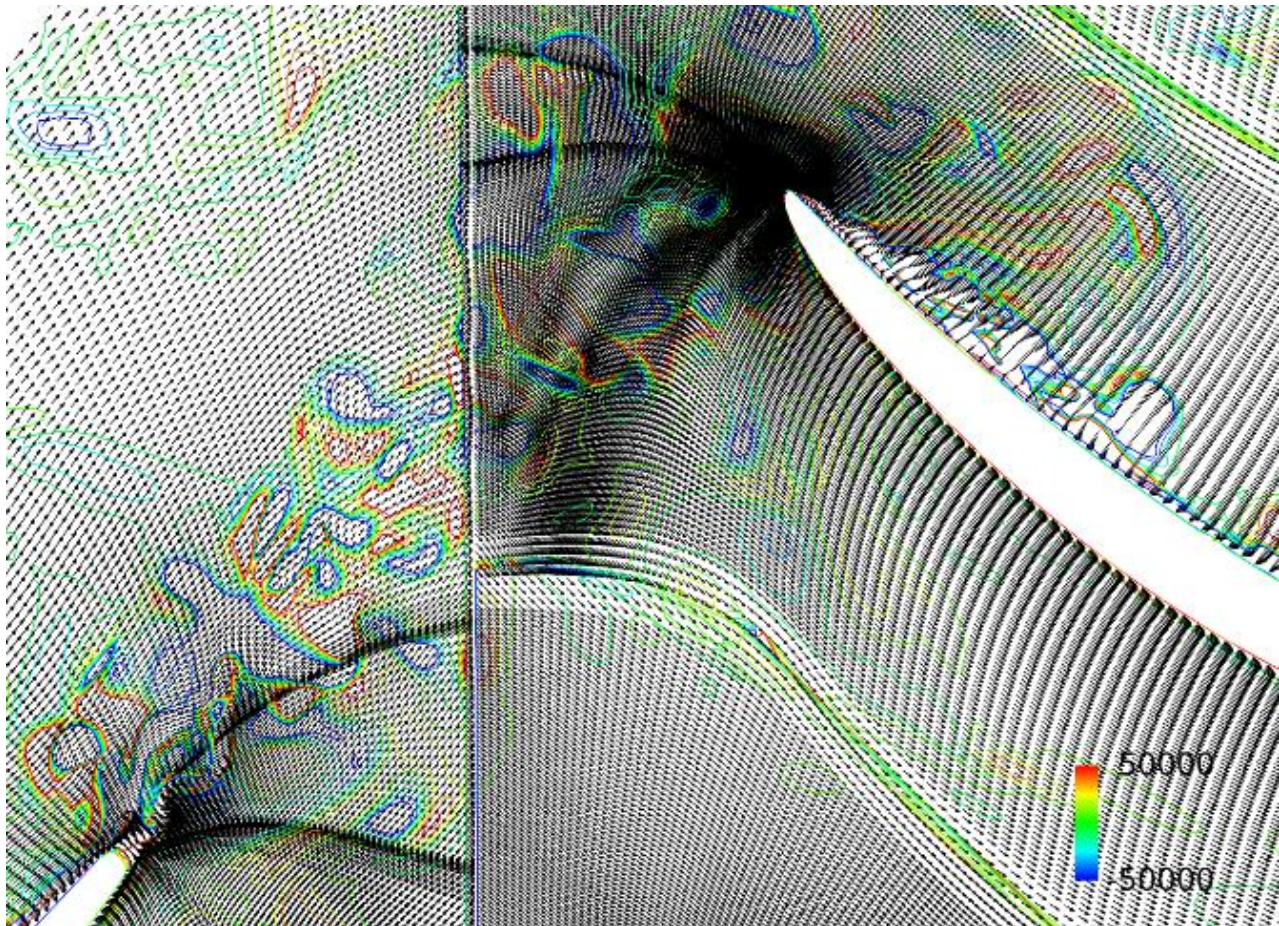
7

Figure 15: Instantaneous velocity vectors and vorticity contours at mid-span from LES

Interaction of rotor wake with the stator blade boundary layer and stretching of rotor wake

Figure 19 shows the instantaneous distribution of total temperature at three different times as the rotor wake passes through the stator. As shown in Figure 8, the rotor wake consists of many vorticities. Instantaneous total temperature distributions in Figure 19 also show many vortical structures with high total temperature. The instantaneous total temperature in the wake is as high as 15 degrees R compared to the total temperature of the non-wake fluid. Instantaneous distribution of total temperature in Figure 19 shows that the total temperature in the rotor wake remains high near the pressure side as it passes through the stator. On the other hand, the fluid with high total

temperature diminishes near the suction side. When averaged over time, the total temperature near the pressure side is about 10 degrees R higher than that near the suction side. Rotor wake entering the suction side and the pressure side of the blade has the same total temperature. Therefore, some redistribution of rotor wake must occur as it passes through the stator passage.

The instantaneous total temperature distribution in Figure 19 shows that the total temperature of the rotor wake remains high near the pressure side as it passes through the stator. On the other hand, the high total temperature spot of the rotor wake diffuses near the suction surface as it passes through the stator. The pressure side of the blade has a concave curvature, while the suction side of the blade has a convex curvature near the leading edge. Effects of longitudinal curvature on
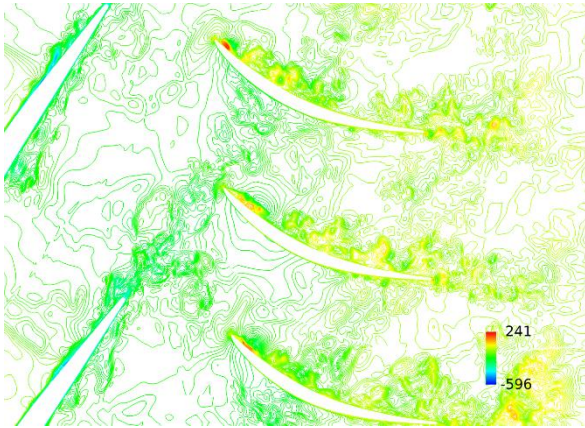
8

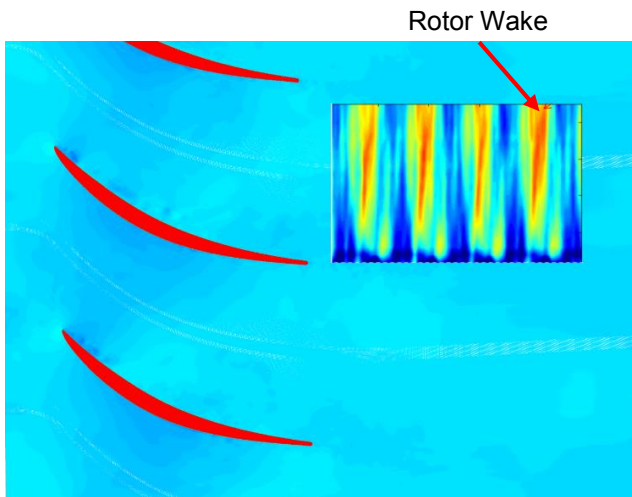**Figure 16: Instantaneous tangential velocity component**

Figure 17: Stator trailing edge total pressure time-space plots at 48.1% span

the stability of a curved wall boundary layer have been studied since Prandtl [1929]. The convex curvature stabilizes the wall boundary layer and the concave curvature has the opposite effect as it increases the turbulent mixing. Due to the effects of longitudinal curvature, more mixing occurs near the pressure side and less mixing occurs near the suction side. This enhanced mixing near the pressure side pulls more rotor wake fluid with a higher total temperature towards the pressure side of the blade. The instantaneous total temperature distribution in Figure 19 shows spots with high total temperature between wakes near the pressure side.

These high temperature spots are due to enhanced mixing near the pressure side.

Instantaneous total pressure near the pressure side in Figure 17 is lower near the pressure side as the rotor wakes interacts with the blade. On the other hand, rotor wakes pass through the stator with less turbulent mixing. The flow between the rotor wakes near the suction surface is cleaner compared to that near the pressure surface. Rotor wakes, which consist of many three-dimensional vortex structures, interact quite differently with the pressure side than with the suction side of the blade. The longitudinal curvature is considered to significantly influence how the three-dimensional vorticities interact amongst themselves. The URANS does not represent vortex interaction and the effects of longitudinal curvature, which might be a reason why URANS does not calculate the current phenomena.

The effects of rotor wake stretching in the stator passage were first studied by Smith [1966]. Stretching of the rotor wake produces total pressure recovery, as explained by Smith [1966]. Soranna et al. [2006] studied the effects of inlet guide vane impingement on the rotor blade experimentally. They observed a negative production of turbulent kinetic energy where some velocity components are stretched. Changes in the vorticity distribution at mid-span of the stator as the rotor wake passes through the stator, found using LES, is given in Figure 20. The vorticity distribution in Figure 20 clearly shows stretching of the rotor wake as it goes through the stator. Most wake stretching occurs near the suction surface as the maximum streamwise velocity occurs near the suction surface. Due to the stretching of the wake, the wake becomes narrower near the suction side and wider near the pressure side, which results in higher averaged total temperature at the stator exit. Furthermore, any possible total pressure recovery by the wake stretching should be realized near the suction side for the current compressor stage.
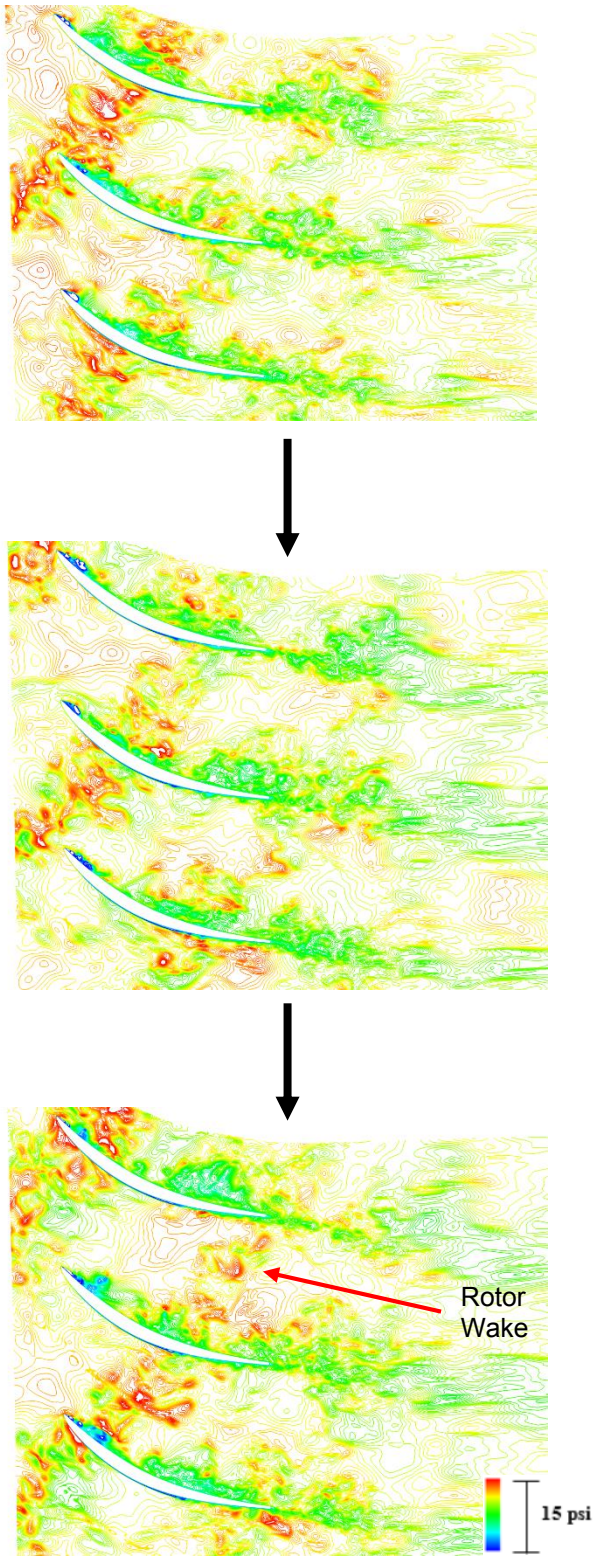
Figure 18: Changes in total pressure distribution at stator mid-span

Rotor Wake

15 psi

CONCLUDING REMARKS

LES is applied to identify possible mechanisms of unsteady loss generation in the stator in an advanced GE highly-loaded, high reaction transonic one and a half stage compressor. The primary focus was to explain why the total temperature becomes higher and why the total pressure becomes lower near the pressure side of the stator. Previous investigations have shown that various tools based on RANS and URANS do not calculate this phenomena correctly. The applied LES calculates higher total temperature with lower total pressure on the pressure side of the stator. Consequently, high loss generation is calculated on the pressure side of the stator as the measured data indicates. Detailed examination of the unsteady flow field by LES reveals following observations:

1. Intra-stator transport of the rotor wake by the jet velocity (Kerrebrock and Mikolajczk [1970]) does not appear to be the main mechanism of the observed high total temperature near the pressure side of the stator. The current LES analysis shows that the jet velocity in the wake decays fast when the wake enters the stator passage. Therefore, most inviscid redistribution of the high temperature wake fluid occurs near the front of the stator passage. If the inviscid intra-stator transport of the rotor wake is the main mechanism of the high total temperature near the pressure side, a simple stage RANS/URANS should be able to calculate the phenomena.

2. The calculated unsteady flow field from a LES shows that flow near the pressure side of the stator is less stable and has a thick boundary layer, even after the rotor wake sweeps through the blade. On the other hand, flow near the suction side is much more stable and has a very thin boundary layer developing even after the rotor wake sweeps the stator blade. Effects of convex and concave longitudinal curvature seem to contribute to the lower total pressure near the pressure side. Additionally, enhanced mixing near the pressure side due to the concave curvature pulls more wake fluid with
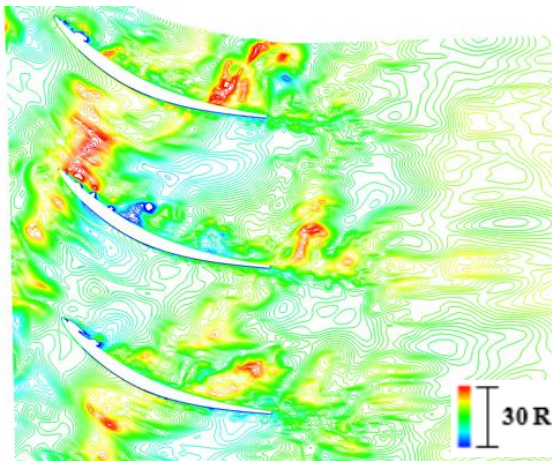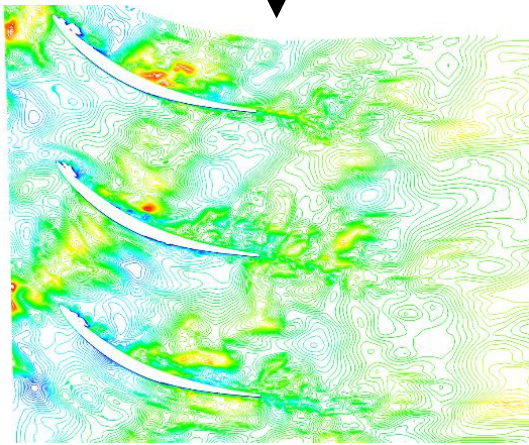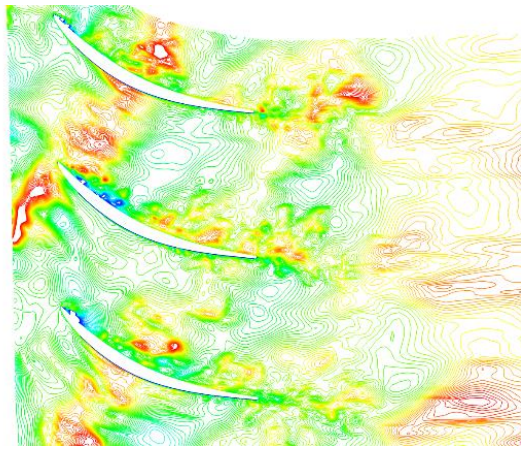
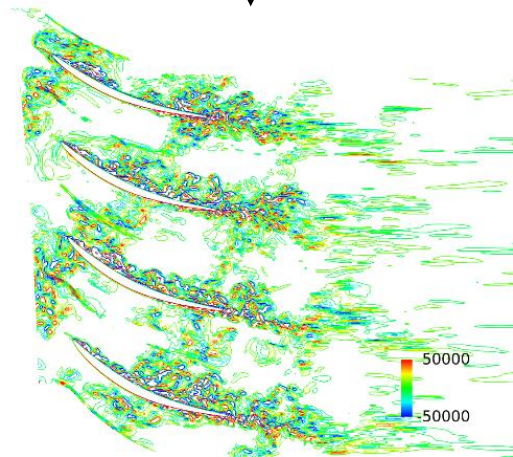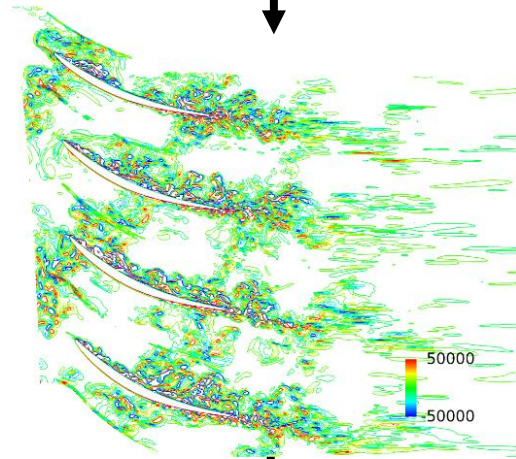**Figure 19: Changes in total temperature distribution at stator mid-span**
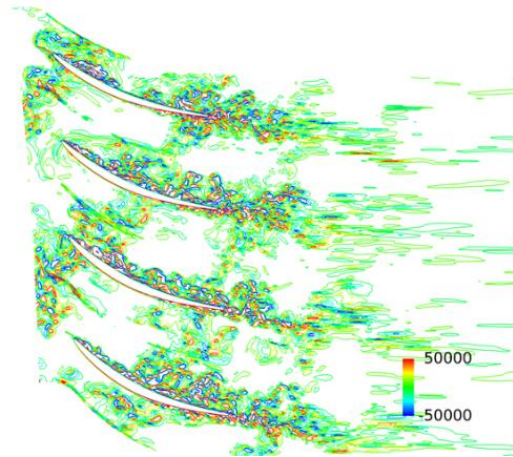

Figure 20: Changes in vorticity distribution at stator mid-span

a high total temperature towards the pressure side.

3. Due to the stretching of the rotor wake through the stator passage, the wake becomes thinner near the suction side and becomes thicker near the pressure side, which contributes to the higher total temperature observed at the stator exit.

REFERENCES
Germano, M., Piomelli, U., Moin, P., and Cabot, W. H., 1991, "A Dynamic Subgrid-Scale Eddy-Viscosity Model," Journal of Fluid Mechanics, Vol. A3, pp. 170-176.

Görtler H., 1954, "On the three-dimensiaonal instability of laminar boundary layers on concave walls," NACA TM 1375.

Gourdain, N., 2013, "Validation of Large Eddy Simulation for the Prediction of Compressible Flow in an Axial Compressor Stage," ASME paper GT 2013-94550.

Hah, C., 2015, "Effects of Unsteady Flow Interactions on the Performance of a Highly-Loaded Transonic Compressor Stage," ASME Paper, GT2015-43389.

Hah, C. and Shin, H., 2012, "Study of Near –Stall Flow Behavior in a Modern Transonic Fan with Compound Sweep," ASME Journal of Fluids Engineering, Vol.134, pp.071101-071107.

Hah C. and Katz J., 2014 "Investigation of Tip Leakage Flow in an Axial Water Jet Pump with Large Eddy Simulation," proceedings of 30th Naval Hydrodynamics Symposium, Hobart, Australia.

Kerrebrock J.L. and Mikolajczk A. A., 1970, "Intra-Stator Transport of Rotor Wakes and Its Effect on Compressor Performance," ASME Journal of Engineering for Power, Vol.92, pp 359-368.

Knobbe, H., and Nicke, E., 1012 "Shock Induced Vortices in Transonic Compressors: Aerodynamic Effects and Design Correlations," ASME Paper, GT2012-69004.

Lurie, D.P. and Breeze-Stringfellow, A, 2015, "Evaluation of Experimental Data from a Highly Loaded Transonic Compressor Stage to Determine Loss Sources," ASME Paper GT2015-42526.

Nolan, S.P.R., Botros, B.B., Tan C.S., Adamczyk, J.J., Greitzer, E.M., and Gorrel, S.E., 2009, "Effects of Upstream Wake Phasing on Transonic Axial Compressor Performance," ASME Paper, GT2009-59556.

Padogiannis, D., Duchane, F., Gicquel, L., Wang, G., and Moreau, S, "Large Eddy Simulation of High Pressure Turbine Stage: Effects of Sub-Grid Scale Modeling and Mesh Resolution," ASME paper GT2014-25876.

Prahst, P.S., Kulkarni, S., and Sohn, K.H., 2015, "Experimental Results of the First Two Stages of an Advanced Transonic Core Compressors Under Isolated and Multi-Stage Conditions," ASME Paper, GT2015-42727.

Prandtl, L., 1929, "Effects of stabilizing forces of turbulence," NACA TM 625.

Smith L. H. Jr., 1966, "Wake Dispersion in Turbomachines," ASME Journal of Basic Engineering, Vol. 88.

Smith L. H. Jr., 2010, Private communication.

To, W., 2015, Private communication.

Soranna, F., Chow, Y., Uzol, O., and Katz, J., 2006, "The Effects of Inlet Guide Vanes Wake Impingement on the Flow Structure and Turbulence around a Rotor Blade," ASME Journal of Turbomachinery, Vol. 128, pp 82-95.

Van Zante, D.E., Adamczyk, J.J., Strazisar, A.J., Okiishi, T.H., 2002, "Wake Recovery Performance Benefit in a High Speed Axial Compressor," ASME Journal of Turrbomachinery, Vol.124, pp275-284.

Zaki, T, Wissink, J., Durbin, P.A., and Rodi, W., 2010, "Direct Numerical Simulations of Transition in a Compressor Cascade: the Influence of Free-Stream Turbulence," J. of Fluid Mechanics, Vol. 665, pp 57- 98.